Molecular and Supramolecular Structures of *N*-Phenyl Formamide and its Hydrated Clusters

John A. Dickinson, Matthew R. Hockridge, Evan G. Robertson, and John P. Simons*

Physical and Theoretical Chemistry Laboratory, South Parks Road, Oxford OX1 3QZ, U.K.

Received: April 19, 1999; In Final Form: June 21, 1999

The amide, *N*-phenyl formamide (formanilide), and its water clusters have been studied in a jet expansion using laser-induced fluorescence excitation and mass-selected, resonant two-photon ionization (R2PI) techniques. The isomer with a trans configuration of the amide group (defined in Figure 1) is identified through analysis of the partially resolved contour of its $S_1 \leftarrow S_0$ band origin. Ion-dip "hole-burn" spectra of the nonplanar cis isomer contain *either* symmetric *or* antisymmetric components of low-frequency progressions, providing evidence of a double-minimum ground state potential. Excited-state vibrations at 76 and 152 cm^{-1}, which are strongly Franck−Condon active, show evidence of Duschinski mixing of the ground-state modes including C_{ring}−N torsion. Water clusters have been observed for *trans*-formanilide only: two distinct 1:1 hydrates, two 1:2 hydrates, and a complex with at least four bound water molecules. (The cis isomer is also expected to form extremely stable complexes with water, but none have been detected experimentally in the present study.) The observed clusters are assigned using spectroscopic data, including band contours, to structural alternatives computed ab initio at the HF/6-31G* level. The 1:1 hydrates are assigned to a cluster in which water binds at the NH site and one in which water binds at the HCO site. In the 1:2 clusters, the addition of a further water molecule to each of the 1:1 clusters results in cyclic hydrogen-bonded structures, with the water dimer bridging between proton donor and proton acceptor sites of the host. The interactions are HCO···HOH and OCH···OH_2 in one case and NH···OH_2 and π_{ring}···HOH in the other. At the MP2/6-31G*//HF/6-31G* level, these structures are ca. 10 kJ mol^{-1} more stable than the nearest competitor, in part because of cooperative effects. The R2PI spectrum of the NH bound 1:2 cluster "C" is very similar to that of the indole$(H_2O)_2$ complex assigned by Zwier and co-workers.[19] Its origin is red-shifted 482 cm^{-1} from *trans*-formanilide, and the electronic transition excites long intermingled vibrational progressions with frequencies of 29, 38, and 51 cm^{-1}.

1. Introduction

Inter- and *intra*molecular hydrogen-bonded interactions are a universal feature of biomolecular architectures, influencing their electronic charge distributions, conformational landscapes, and *supramolecular* structures. There is a subtle balance between *intra*molecular and *inter*molecular bonding, for example, between an amide group and neighboring groups on a peptide chain, or an amide group and neighboring solvent molecules, such as water. In reaching the balance, their individual contributions need not be additive; cooperative interactions may make the whole more than the sum of the parts.[1]

Although there are a *plethora* of theoretical predictions,[1−3] usually based upon SCF calculations, of the preferred *supra*molecular structures of hydrated amide groups, experimental measurements have almost always been indirect. Typically, they have been based upon a theoretical interpretation of the infrared,[4,5] resonance Raman[6] or NMR[7,8] spectra of model systems such as formamide (the simplest example), or *N*-alkyl or *N*-phenyl amide−water clusters, either isolated in a matrix or dispersed in an aqueous solution. Direct structural investigations of *isolated* hydrated amide clusters are hard to find. but some notable exceptions are studies of the formamide water cluster by microwave spectroscopy[9] and of the cyclic amide, 2-pyridone, by laser-induced fluorescence excitation (LIF) spectroscopy.[10] This latter study, conducted at rotational levels of resolution by Held and Pratt, has enabled the assignment of bridged *supra*molecular structures to both its 1:1 and 1:2 hydrates, isolated in the low-temperature environment of a free-jet expansion. Small changes in the C−N and C═O bond lengths imply a polarization of the electron distribution in the hydrated amide group.[1]

Until recently, this exploration of the correlation between the *supra*molecular structures of the clustered water molecules and the conformational and electronic structures of the organic molecules to which they were bound, represented a unique study. The incorporation of the amide group in the cyclic structure of 2-pyridone, which forces it into a cis configuration, makes it an even more special case. In the absence of the cyclic constraint, the trans configuration would have been preferred. In *N*-phenyl formamide (formanilide), the cis and trans configurations have comparable stabilities; both can be isolated in a free jet expansion and their (unhydrated) structures have been explored recently by Cable and co-workers.[11] Resonantly, enhanced two-photon ionization (R2PI) spectra, recorded at vibrational resolution only, but supported by ab initio and semiempirical calculations, allowed them to assign planar and twisted equilibrium geometries, respectively, to the trans and cis amide configurations, as defined in Figure 1.

In general, free jet expansion, coupled with LIF or R2PI detection and rotational band contour analysis, provides a powerful strategy for probing both conformational and *supra*molecular structure.[10−16] It becomes even more powerful when

10.1021/jp991254d CCC: $18.00
Published on Web 08/18/1999

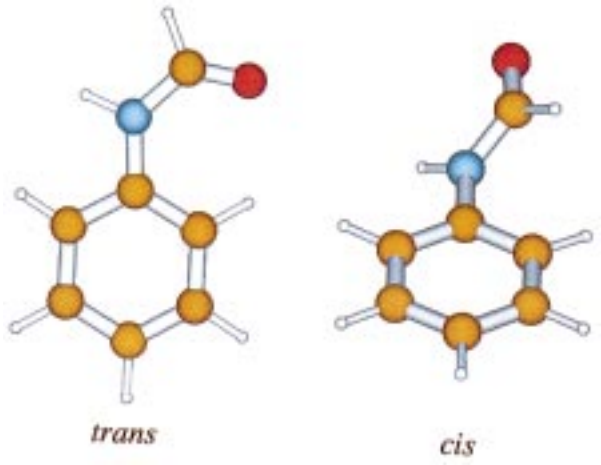

Figure 1. Isomers of formanilide predicted by MP2/6-31G* calculations.

it is reinforced by ion-dip spectral "hole-burning" experiments, in the ultraviolet[17] and/or in the infrared.[18,19] Mass-selected detection permits the identification of size-selected hydrated clusters (as well as their molecular hosts), while the "hole-burning" experiments enable their spectral features to be separately isolated. Structural assignments can be achieved through analysis of the rotational and/or vibrational band contours of the isolated features, aided crucially by the predictions of ab initio computation.

Over the past few years, we have exploited these strategies to determine the conformational and *supra*molecular hydrate structures of the carboxylic acid 3-phenyl propionic acid;[20] the neurotransmitter 2-phenylethylamine together with 2-phenyl ethanol[21,22] and its *p*-hydroxy derivative, the antioxidant *p*-tyrosol;[23] and the enzyme inhibitor, 4-phenylimidazole (4-PI), and its tautomer, 5-PI.[24] In each of these molecules, the benzene (or phenol) ring provides the optical "antenna" (through the $S_1 \leftarrow S_0$, $\pi \rightarrow \pi^*$ transition), and the flexible side chain provides the conformational variety. Conformational and structural assignments have been greatly facilitated by the discovery of a strong sensitivity of the $\pi \rightarrow \pi^*$ electronic transition dipole orientation, reflected in the rotational band contour, to the conformation and "chemical" structure of the side chain and to its local molecular environment, e.g., the local hydration shell.[20−27]

In the present work, the strategies are used to explore and characterize the conformational and supramolecular hydrate structures of the model peptide formanilide. The new work enhances and greatly extends the earlier studies reported by Cable and co-workers,[11] to include: (a) the structural assignment of its (planar) trans isomer, based upon a rotational analysis of its $S_1 \leftarrow S_0$ origin band contour, aided by high-level ab initio computation, (b) a selective spectral "hole-burning" experiment which signals the splitting of the zero-point level of the (twisted) cis isomer into symmetric and antisymmetric components by potential barriers along the torsional and bending coordinates, located at the coplanar configuration, and (c) a revised vibrational analysis of the low-frequency progressions observed in the ultraviolet spectrum of *cis*-formanilide, again supported by ab initio computation.

Most importantly, rotational and/or vibrational band contour analyses and ab initio calculations have enabled assignments to be reported, for the first time, of the supramolecular structures of isomeric pairs of singly, and doubly, hydrated clusters of *trans*-formanilide, distinguished through fluorescence excitation, mass-selected R2PI and ion-dip, ultraviolet hole-burning spectroscopy.

The paper is organized as follows. The analytical and experimental procedures are described in section 2, and new experimental data for the isolated isomers of formanilide are presented and analyzed to provide secure structural assignments in section 3. Electronic spectra of a number of singly, doubly, and multiply hydrated clusters of (trans) formanilide are presented in section 4, and structural assignments are proposed in light of ab initio calculations, rotational band contour analysis, vibrational analysis, and the interpretation of the observed spectral shifts. Section 5 provides a commentary on the results and their significance in a wider context.

2. Analytical and Experimental Procedures

2.1. Molecular Orbital Calculations. Possible structures of formanilide and its 1:1 and 1:2 water clusters were explored by performing a series of ab initio molecular orbital calculations using Gaussian 94[28] as follows.

(i) A set of starting geometries was generated for formanilide and its clusters. The formanilide molecule was given a planar arrangement of the amide bond, for both cis and trans isomers, while the dihedral angle τ_{C2C1NC} was varied to allow both planar and nonplanar molecular structures. For 1:1 water clusters, the geometry of the host molecule was initially set to each optimized structure attained in the absence of any solvent molecules. A set of structures was then generated in which a water molecule was bound to the N−H hydrogen, or to "lone pair" sites of the carbonyl group, or at bridging sites between the amide group and the π-system of the ring. Initial structures for 1:2 water clusters were based on optimized 1:1 structures for the cis and trans isomers. The second water molecule was either connected solely to the first via a "linear" hydrogen bond, located at one of the alternative amide binding sites, or inserted into the cluster to allow a cyclic hydrogen-bonded network, with a C−H site acting as a proton donor, for example. Extensive testing of different starting geometries was performed to locate all potential minima associated with two water molecules bound to the amide group.

(ii) Each geometry was then submitted to full ab initio optimization at the HF/6-31G* level of theory. In cases where only one of the hydrogen atoms of the water molecule was bound to the host, the other hydrogen atom was rotated stepwise by 120° about the molecular OH axis and the resulting structure was reoptimized to find any further local minima.

(iii) Force fields were calculated at the HF/6-31G* level for each optimized structure, to ensure that they represented true potential minima and to obtain zero-point energy corrections.

(iv) Basis set superposition errors (BSSE) were calculated to include the fragment relaxation energy,

$$E_{BSSE} = E_{AB}^{\alpha}(A) - E_{AB}^{\alpha\cup\beta}(A) + E_{AB}^{\beta}(B) - E_{AB}^{\alpha\cup\beta}(B) \quad (1)$$

$E_{AB}^{\alpha\cup\beta}(A)$ is the electronic energy of fragment A in the geometry of the complex AB with the complex basis set $\alpha\cup\beta$.

(v) MP2/6-31G* single-point calculations were performed using the HF/6-31G* optimized geometry. The two stable molecular conformations were also reoptimized at the MP2/6-31G* level.

(vi) Ground state structures were subsequently optimized for the first electronically excited singlet state, at the CIS/6-31G* level of theory, to yield sets of rotational constants for the electronically excited S_1 state of each isomer, together with the magnitudes and directions of the $S_1 \leftarrow S_0$ transition moment (TM).

2.2. Mass-Selected R2PI, Ion-Dip Hole-Burning, and LIF Spectroscopy. Mass-selected, one-color R2PI spectra were recorded at low resolution (ca. 0.5 cm^{-1}) using a YAG-pumped, frequency-doubled dye laser (LAS) operating at wavelengths ca. 270−290 nm. Jet-cooled samples were introduced through a pulsed nozzle helium expansion system (General Valve, series 9, 0.5 mm orifice, stagnation pressure 2−4 bar, sample temperature 350−390 K), and the ion signals were detected via a differentially pumped time-of-flight mass spectrometer (R.M. Jordan). When required, water vapor was incorporated into the gas flow via a bypass system. Hole-burn ion-dip spectra were recorded using a double resonance optical configuration. The burn laser radiation was provided by a YAG-pumped laser (Lambda-Physik, FL3002) which was scanned through the band origin region; the second, counterpropagating "probe" laser (LAS), delayed by 260 ns, was tuned to a series of fixed frequencies associated with selected features in the R2PI spectrum. Finally, LIF spectra were recorded at higher resolution, to provide partially resolved rotational band contours, by etalon-narrowing the frequency-doubled, excimer-pumped, dye laser output to a line width ca. 0.08 cm^{-1} and substituting an optically filtered photomultiplier for the mass spectrometric detection system. The nozzle diameter employed in these experiments was 0.8 mm.

2.3. Rotational Band Contour Analysis. Simulated band contours, based on a rigid, asymmetric rotor Hamiltonian, were fitted to experimental contours using a program based on correlation analysis.[23,27] It uses a simple golden section search routine to optimize the values of the rotational constants $(A-\bar{B})''$ and $(A-\bar{B})'$, $\bar{B}''$, and $(B-C)''$, the rotational temperature, and the experimental resolution, by maximizing the value of the correlation coefficient with respect to each parameter in turn. $\bar{B}''$ and $(B-C)''$ were constrained to the ground-state values, since the experimental band contours were recorded at a resolution insufficient to allow determination of all six rotational constants. A two-dimensional simplex method was employed to optimize the band hybrid character, with the two optimization parameters being the proportions of *a* and $b/(b + c)$ type character.

3. Formanilide

3.1. Ab Initio Calculations. At both HF/6-31G* and MP2/6-31G* levels, two isomers were found with almost identical stabilities. *Trans*-formanilide (*t*-FA) is planar and *cis*-formanilide (*c*-FA) is nonplanar, with $\tau_{C2C1NC} = 42°$, consistent with Cable's calculations at levels up to HF/6-31G*.[11] The CIS/6-31G* optimizations resulted in planar structures for the electronically excited S_1 state of both isomers, and the magnitude and the alignment of their $S_1 \leftarrow S_0$ transition dipole moments (in the geometry of the ground state) were very similar. Molecular parameters obtained from the ab initio calculations on formanilide are summarized in Table 1.

3.2. Electronic Spectroscopy. One-color R2PI spectra of formanilide and associated water clusters in the $S_1 \leftarrow S_0$ origin region are shown in the upper trace of Figure 2. Under nonclustering conditions, the spectrum in the monomer mass channel shows two distinct sets of features: an extended vibrational progression starting at "A" (34 912 cm^{-1}), and an intense peak labeled "B" (at 36 001 cm^{-1}), accompanied by several weaker, blue-shifted features.

A hole-burn spectrum, probing depletion of the monomer peak "B", is shown in the lower trace of Figure 2. It contains all the features present in the blue-shifted region of the R2PI spectrum under nonclustering conditions, confirming their association with a single molecular conformer. The rotational contour of band "B", obtained by fluorescence excitation, is shown in Figure 3, together with contours predicted from ab initio data for cis and *trans*-formanilide. The ab initio contour for *trans*-formanilide matches the experimental spectrum extremely well. Comparison of the ab initio parameters for both isomers with those obtained using the cross-correlation fitting procedure described in section 2 confirms the assignment of band "B" to *trans*-formanilide (see Table 2). Obtaining a fluorescence excitation contour of the "A" origin was difficult due to strong resonant (and nonresonant) fluorescence from aniline, a thermal decomposition product.

The extended, low-frequency progressions in the red-shifted band system, A, are consistent with their earlier assignment by Cable[11] to *cis*-formanilide, the isomer predicted by ab initio calculations to undergo a large geometry change on excitation. Figure 4 displays hole-burning spectra in the red-shifted region, with the two lower traces showing the ion depletion signal in the first two members of the progression as the burn laser is scanned. The two spectra are not identical, indicating that the first two members of the progression do not share a common lower state. The same phenomenon was observed very recently in 5-phenylimidazole,[24] where the analogous hole-burn spectra displayed *either* even *or* odd members only, of a low-frequency torsional progression. The imidazole ring is twisted relative to

TABLE 1: Molecular Parameters Predicted from HF/6-31G*, MP2/6-31G*, and CIS/6-31G* Calculations on Formanilide Conformers

	t-FA	*c*-FA
E_{rel}[a]/kJ mol^{-1}	0.2	0.0
τ_2 ($C_2C_1NC_\pi$)/deg[b]	0.0	42.6
τ_3 ($C_2C_1NC_\pi$)/deg[c]	0.0	6.5
A''/MHz	4200.9	5014.5
B''/MHz	1120.6	925.6
C''/MHz	884.6	795.1
A'/MHz	4183.2	4943.2
B'/MHz	1118.4	949.3
C'/MHz	882.5	798.0
$\lvert R_e \rvert \times 10^{30}$/$Cm^4$	2.54	2.52
$\mu_a^2/\mu_b^2/\mu_c^{2d}$	13:87:0	2:98:1
θ_{elec}/deg[d]	+2.9	−1.1

[a] MP2/6-31G* + 0.9(zero-point correction). Correction taken from HF/6-31G* calculation. [b] S_0 interplane torsional angle. [c] S_1 interplane torsional angle (S_1 calculations at CIS/6-31G* level). [d] Transition parameters calculated at S_0 MP2/6-31G* optimized geometry. θ_{elec} is defined as the TM rotation angle in the plane of the benzene ring, away from the short axis. A positive rotation represents an anticlockwise movement.

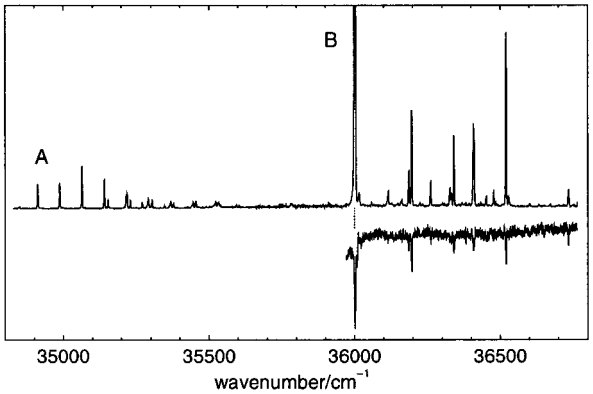

Figure 2. Upper trace: Mass-selected one-color R2PI spectrum of formanilide under nonclustering jet conditions. Lower trace: R2PI hole-burning spectrum, probing depletion of the peak labeled "B".

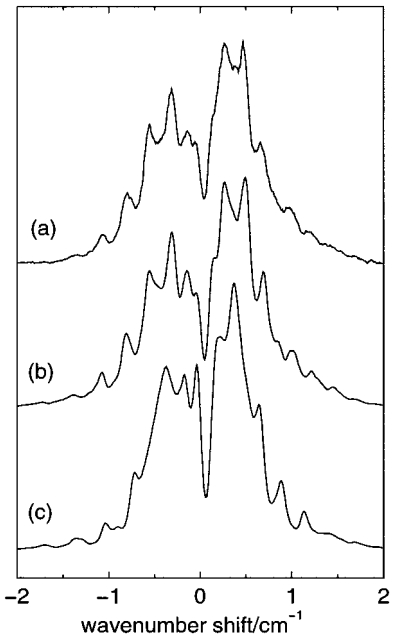

Figure 3. (a) Fluorescence excitation contour of band B. Below are simulated contours based on ab initio data for (b) trans and (c) cis formanilide given in Table 1 (T_{rot} = 2 K, fwhh = 0.08 cm^{-1}).

TABLE 2: Observed and Predicted Parameters Relating to the $S_1 \leftarrow S_0$ Band Origin B in Formanilide

	band origin cm^{-1}	(A−B̄)″ cm^{-1}	B̄″ cm^{-1}	(B−C)″ cm^{-1}	$\mu_a^2/\mu_b^2/\mu_c^2$	E_{rel} kJ mol^{-1}[a]
B	36001	0.1034	0.0267	0.0035	31:64:5	
t-FA		0.1066	0.0335	0.0079	13:87:0	0.2
c-FA		0.1386	0.0287	0.0044	2:97:1	0.0

[a] MP2/6-31G* + 0.9*(zero-point correction from HF/6-31G*).

the phenyl ring in the ground state of 5-phenylimidazole, and as a result, each torsional level in the ground electronic state is split into symmetric and antisymmetric components by tunneling through the coplanar potential barrier. In contrast, the upper electronic state has a planar (or near planar) equilibrium geometry and the successive torsional levels, which alternate between even (symmetric) and odd (antisymmetric) parity, are therefore selectively excited from the two ground-state levels. The *cis*-formanilide hole-burn spectra, shown in Figure 4, may be explained in a similar manner, but with the added complication that there are now two low-frequency modes in the S_1 state which show strong Franck−Condon activity.[11] We have labeled them, ν_A (76 cm^{-1}) and ν_B (152 cm^{-1}), and the principal assignments are listed in Table 3. Transitions that excite multiple

TABLE 3: Vibronic Transition Assignments of Formanilide Cluster "A"

transition energy $\bar{\nu}$/cm^{-1} − 34912	present in s/a spectrum	assignment
0.0	s	$A_0^0B_0^0$
75.0	a	$A_0^1B_0^0$
151.7	s	$A_0^2B_0^0$
151.8	a	$A_0^0B_0^1$
228.1	a	$A_0^3B_0^0$
228.6	s	$A_0^1B_0^1$
302.7	s	$A_0^4B_0^0$
303.6	a	$A_0^2B_0^1$
306.5	s	$A_0^0B_0^2$
377.4	s	$A_0^3B_0^1$
379.9	a	$A_0^1B_0^2$
451.8	a	$A_0^4B_0^1$
454.6	s	$A_0^2B_0^2$
457.6	a	$A_0^0B_0^3$
526.8	s	$A_0^5B_0^1$
530.6	a	$A_0^3B_0^2$
533.8	s	$A_0^1B_0^3$
600.8	a	$A_0^6B_0^1$
605.0	s	$A_0^4B_0^2$
608.7	a	$A_0^2B_0^3$
611.6	s	$A_0^0B_0^4$
241.4	a	C_0^1
358.3	s	D_0^1

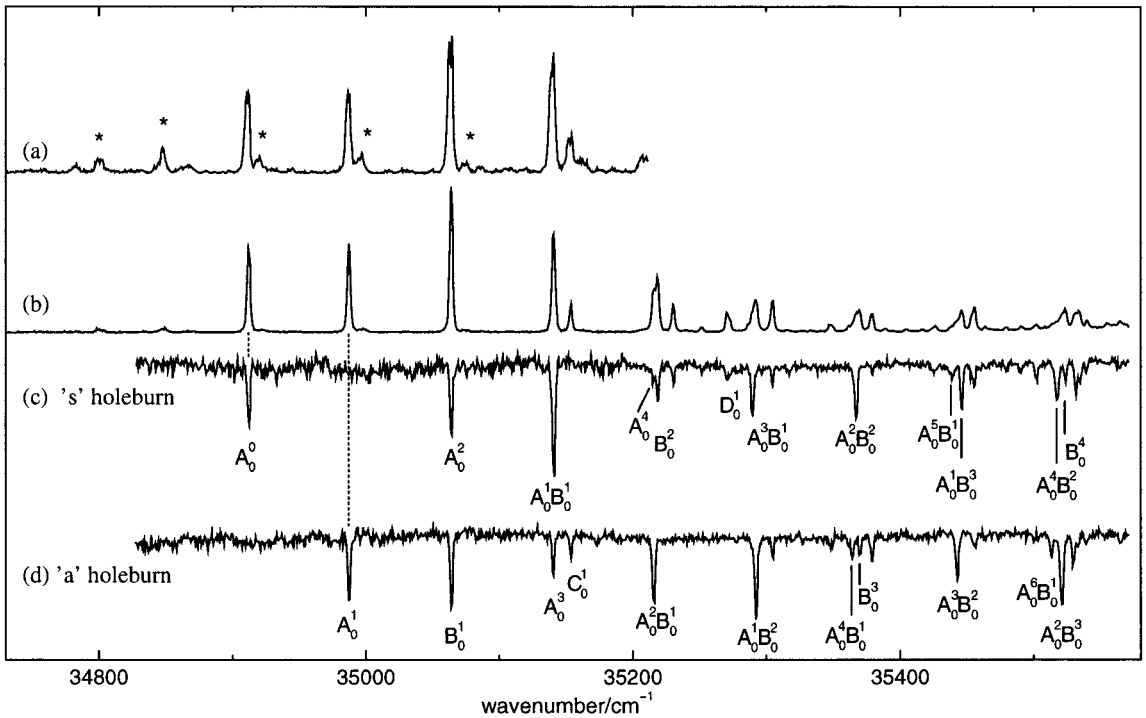

Figure 4. Mass-selected one-color R2PI spectra of formanilide in the region of isomer "A", under (a) warm and (b) cool expansion conditions. Below are R2PI hole-burning spectra, probing depletion of (c) the peak labeled "A_0^0" and (d) the peak labeled "A_0^1". The features marked * are assigned as hot bands.

quanta of these modes are overlapped in the R2PI spectrum since the frequency of ν_B is almost exactly twice that of ν_A. Their contributions were separated, however, by Cable et al.,[11] who measured the spectrum of formanilide-d_5, where the two frequencies are shifted enough to allow resolution of the nearly coincident vibronic transitions. In our experiments, the overlapping R2PI transitions (in the *undeuterated* molecule) are distinguished through the separate "s" and "a" hole-burn spectra shown in Figure 4, which depend on the symmetry of their vibrational wave functions with respect to the molecular plane. The A_0^1 and B_0^1 transitions both appear in the "a" spectrum, for example, while A_0^2 appears in the "s" spectrum. Later in the progression, when neighboring transitions may have the *same* excited-state symmetry, e.g., the combination and overtone bands, $A_0^4B_0^1$ and B_0^3, they *can* be resolved in the hole-burning spectra. Either ν_A and ν_B have different anharmonicities or the levels are split by Fermi resonance interactions.

Clues to the nature of ν_A and ν_B may be found by examining the spectra and the ab initio calculations together. The latter indicate a change in geometry following excitation from S_0 to S_1, associated principally with twisting about the C_1-N bond ($\tau_{C2C1NC} = 42.3°$ and 42.6° at HF and MP2 and 6.5° at CIS levels). There is also a small change in the angle τ_{C1NHC} (7.1°, 9.3° at HF, MP2 and 1.2° at CIS levels). This should imply a strong contribution from the C_1-N torsion together with a much smaller contribution from out-of-plane bending about the nitrogen (the remaining low-frequency motion, torsion about $N-C_{amide}$, is not involved). The HF frequencies (scaled by 0.9) associated with these motions are 143 cm^{-1} for the torsion about C_1-N, 65 cm^{-1} for the out-of-plane bend (and 119 cm^{-1} for the torsion about $N-C_{amide}$). In practice, however, the strongest transitions are combination bands exciting approximately equal quanta of ν_A and ν_B. The overtones, A_0^4 and B_0^4, are quite weak, while transitions such as A_0^5 and A_0^6 are so weak they are not seen at all in the hole-burn spectra. This pattern of intensities suggests Duschinski mixing of the S_1 vibrational modes relative to those of S_0. The S_1 vibrational modes, ν_A and ν_B, involve a mixture of C_1-N torsion and at least one other mode of equivalent symmetry with respect to the planarity of the ring. The most likely candidate for a second coupled mode is the out-of-plane bend about the nitrogen, as it involves a very similar motion of the amide C═O group relative to the ring. The two equivalent modes in styrene also show significant Duschinski mixing,[29] although styrene differs from *cis*-formanilide in having a planar geometry in the ground electronic state.

In addition to ν_A and ν_B, weak transitions involving other modes can also be identified in the spectrum, such as the small peaks displaced 241 and 358 cm^{-1} from the origin. Their symmetries with respect to the molecular plane are revealed by their appearance in the "a" and "s" hole-burn spectra, respectively. They are the first members of further progressions exciting ν_A and ν_B, which again alternate between the "a" and "s" spectra in a fashion similar to the main progressions.

4. Formanilide Water Clusters

4.1. Ab Initio Calculations. Optimized structures of 1:1 water clusters of *cis*- and *trans*-formanilide are shown in Figure 5, and their molecular parameters and binding energies (including zero-point and BSSE corrections) are summarized in Table 4. When two alternative structures are found, which vary *only in the orientation of a nonbonded water hydrogen atom*, only the more stable one is presented. The arrows in Figure 5 show the alignment of the TM in the molecular frame, described by the angle θ_{elec} (the angle between the short axis of the benzene ring perpendicular to the $C_{ring}-N$ bond, and the TM). They show some variation, reflecting the influence of the bound water molecule at the different sites, for example, *t*-FA(H_2O) **II** and *c*-FA(H_2O) **II**, which place the water molecule furthest from the aromatic ring, have the smallest values of θ_{elec}. The distinctive (and helpful) differences in the predicted band contours, shown in Figure 5, reflect changes in the TM alignments as well as the rotational constants of the hydrated clusters.

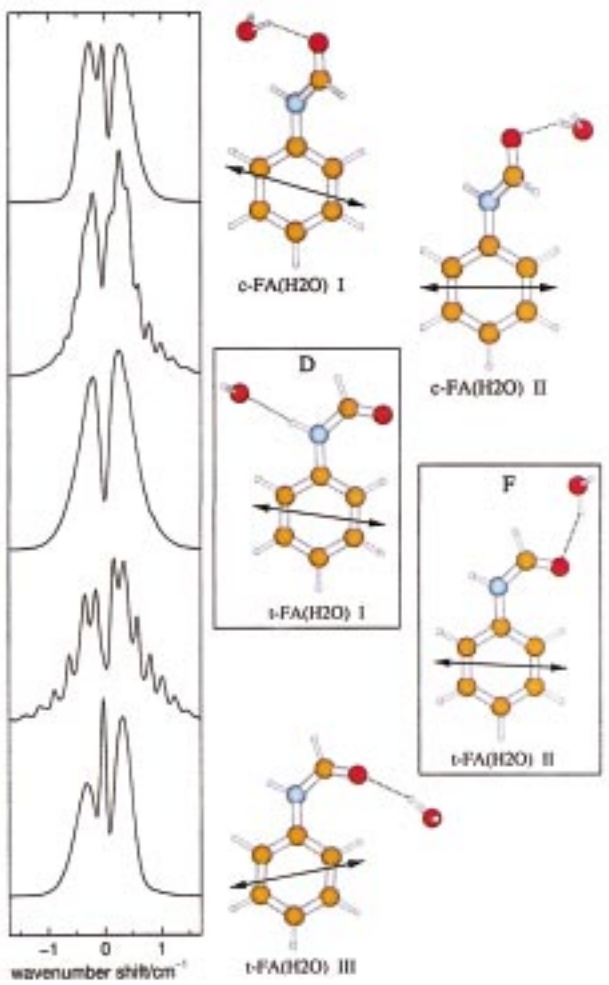

Figure 5. Simulated rotational band contours for the FA(H_2O) complexes shown alongside, on the basis of the ab initio data detailed in Table 4 ($T_{rot} = 2$ K, fwhh = 0.10 cm^{-1}). The boxes indicate structures assigned to experimentally observed clusters D and F.

The most stable 1:1 cluster of *trans*-formanilide is predicted to be *t*-FA(H_2O) **I**, with water bound as a proton acceptor at the N−H site. At the MP2/6-31G*//HF/6-31G* level, the two complexes with water bound as a proton donor to the carbonyl oxygen are ca. 3−5 kJ mol^{-1} less stable; of these, *t*-FA(H_2O) **II**, which benefits from a secondary interaction between the water oxygen and the $H-C_{amide}$, is slightly preferred over *t*-FA(H_2O) **III**. In this third cluster, steric hindrance to the placement of the water molecule induces some nonplanarity in the host molecule, with $\tau_{C2C1NC} = 14°$.

A cis conformation of the amide group allows for an extremely stable cyclic water complex, *c*-FA(H_2O) **I**, with water acting as both proton donor to the carbonyl oxygen and as proton acceptor to the amine hydrogen. Indeed, this type of structure has already been identified through analysis of the microwave spectrum of the 1:1 hydrate of formamide.[9] The binding energy

TABLE 4: Molecular Parameters Predicted from HF/6-31G*//MP2/6-31G* and CIS/6-31G* Calculations on Formanilide 1:1 Water Clusters

water cluster	*t*-FA(H_2O) **I**	*t*-FA(H_2O) **II**	*t*-FA(H_2O) **III**	*c*-FA(H_2O) **I**	*c*-FA(H_2O) **III**
E_{rel}[a]/kJ mol^{-1}	12.7	16.0	18.2	0.0	17.4
E_{bind}[b]/kJ mol^{-1}	22.4	19.6	17.4	31.4	20.4
E_{bind}[c]/kJ mol^{-1}	17.8	12.5	10.4	22.1	13.1
E_{bind}[d]/kJ mol^{-1}	26.0	20.3	18.2	36.2	20.8
$\tau_5(C_2C_1NC_\pi)$[e]/deg	0.0	1.0	13.9	42.1	41.1
$\tau_6(C_2C_1NC_\pi)$[f]/deg	0.0	0.5	6.2	5.5	4.6
A″/MHz	1630.4	4204.6	1869.3	2791.8	2943.3
B″/MHz	900.2	534.3	842.0	657.9	555.5
C″/MHz	581.5	474.6	583.5	552.5	485.8
A′/MHz	1641.9	4113.1	1847.9	2665.7	3029.2
B′/MHz	891.5	531.0	826.9	692.2	561.8
C′/MHz	579.3	470.8	572.8	551.5	475.2
$\lvert R_e\rvert \times 10^{30}$/Cm[g]	2.70	2.24	2.13	2.44	2.20
$\mu_a^2/\mu_b^2/\mu_c^2$[g]	15:85:0	12:88:0	72:28:0	13:77:10	13:74:13
θ_{elec}/deg[g]	−8.5	−2.8	+12.0	−16.1	+0.2
r(N−H···OH_2)/pm	206.6			211.6	
r(C═O···H−OH)/pm		204.9	205.4	205.0	203.4
r(H_2O···H−$C_{C=O}$)/pm		271.9			274.1
r(H_2O···H−C_{ortho})/pm			266.7		

[a] MP2/6-31G*//HF/6-31G* + 0.9(zero-point correction). Corrections taken from HF/6-31G* calculation. [b] HF/6-31G* + 0.9(zero-point correction). [c] HF/6-31G* + 0.9(zero-point correction) + BSSE correction. [d] MP2/6-31G*//HF/6-31G* + 0.9(zero-point correction + BSSE correction. Corrections taken from HF/6-31G* calculation. [e] S_0 interplane torsional angle. [f] S_1 inter-ring torsional angle (S_1 calculations at CIS/6-31G* level). [g] Transition parameters calculated at S_0 HF/6-31G* optimized geometry. θ_{elec} is defined as the TM rotation angle in the plane of the benzene ring, away from the short axis.

at the MP2/6-31G*//HF/6-31G* level is 36 kJ mol^{-1}, which is twice that of the water dimer calculated at the same level of theory (18 kJ mol^{-1}). The NH···OH_2 and CO···HOH hydrogen bond lengths are similar to the corresponding values in *t*-FA complexes, although the hydrogen bond angles are more distorted. The alternative complex of *cis*-formanilide, *c*-FA(H_2O) **II**, has water bound to the carbonyl oxygen in an identical manner as *t*-FA(H_2O) **II**. In neither case does hydration change the degree of nonplanarity of the host molecule, *cis*-formanilide.

Optimized structures and corresponding molecular parameters of 1:2 water clusters of formanilide are shown in Figure 6 and Table 5. They result from an exhaustive search for local potential energy minima of clusters subject to the constraint that each water molecule is bound either to the amide group or to the other water molecule. In structures where a "dangling" (non-bonded) hydrogen of water can adopt two alternative orientations only the more stable alternative is shown. Structures in which the water dimer binds to formanilide via the NH site only converged to the cyclic hydrates, *c*-FA(H_2O)$_2$ **IV** or *t*-FA(H_2O)$_2$ **I**, with the second water bridging to the aromatic ring. Indeed, the most stable structures are those which allow a water dimer to bridge between a proton acceptor site and a proton donor site, to allow three hydrogen-bonded interactions, each of which is strengthened through the effects of cooperation. The *cis*-formanilide cluster, *c*-FA(H_2O)$_2$ **I**, in which the water molecules bridge between the NH and CO sites, is favored by a large margin. Similarly, the most stable *trans*-formanilide clusters are *t*-FA(H_2O)$_2$ **I**, where the water molecules bind to the NH hydrogen and to π-electron density on the ring, and *t*-FA(H_2O)$_2$ **II**, where the two water molecules bridge across the HCO group.

Positive cooperative effects are reflected in increased binding energies and shortened hydrogen bond lengths. One of the complexes in which these effects are most easily isolated is *t*-FA(H_2O)$_2$ **VII**, which has one water molecule bound to the carbonyl oxygen (in fashion very similar to the 1:1 cluster, *t*-FA(H_2O) **II**) and the second water molecule linked to the first, as a proton donor. The increased acidity of the first water molecule in the doubly hydrated cluster shortens the CO···HOH bond length to 196 pm (compared with 205 pm in the 1:1 cluster), but the distance OCH···OH_2 increases from 272 to 299 pm. The binding energy of 43 kJ mol^{-1} is 5 kJ mol^{-1} greater than the total obtained by summing the binding energies of *t*-FA(H_2O) **II** and the water dimer (calculated at the MP2/6-31G*// HF/6-31G* level with HF BSSE corrections). The effects of positive and negative cooperation are also observed acting through the amide molecule in structures with two separate binding sites occupied. In the *t*-FA(H_2O)$_2$ **V** cluster, the NH···OH_2 and CO···HOH hydrogen bond lengths are shortened by 2 and 4 pm relative to the corresponding 1:1 clusters and the binding energy is 2.6 kJ mol^{-1} greater than the sum of the individual binding energies for each 1:1 cluster. In *t*-FA(H_2O)$_2$ **VIII**, with both carbonyl sites occupied, the CO···HOH hydrogen bonds increase by 1 and 6 pm and the binding energy *decreases* by 2.8 kJ mol^{-1} relative to the sum of the individual binding energies. Guo and Karplus noted similar trends in a detailed ab initio study of cooperative effects in *N*-methylacetamide.[1]

The structural changes induced in the host molecule by the addition of one or two bound water molecules are mostly quite small. Changes in the amide bond lengths, N−H, N−C, or C═O, for example, are generally ca. 1 pm. Clusters with water molecules bound in close proximity to aromatic ring hydrogen atoms provide notable exceptions. In the hydrated clusters, *t*-FA(H_2O)$_2$ **III** and **IV**, distortion of the planar amide geometry to permit interactions between water oxygens and ring hydrogens twists the dihedral angle τ_{C2C1NC} from 0° (in the trans monomer) to 35° and 46°, respectively. Similar interactions in *c*-FA(H_2O)$_2$ **II,** reduce the dihedral angle from 42° (in the monomer) to 31°, but there is no evidence for structures in which the two bound water molecules polarize the amide bond sufficiently to induce planarity in the ground state.

4.2. Cluster Stoichiometry. The R2PI and hole-burning spectra, shown in Figures 7 and 8, reveal the presence of five distinct hydrated clusters of formanilide. The features labeled D, E, and F in the FA(H_2O)$^+$ mass channel are associated with three distinct cluster species. Under one-color ionization conditions, species D and F partially fragment into the FA$^+$ mass channel (with efficiencies of ca. 25% and 60%, respectively, although these percentages may be affected by three-photon excitation processes), suggesting their assignment to 1:1 water

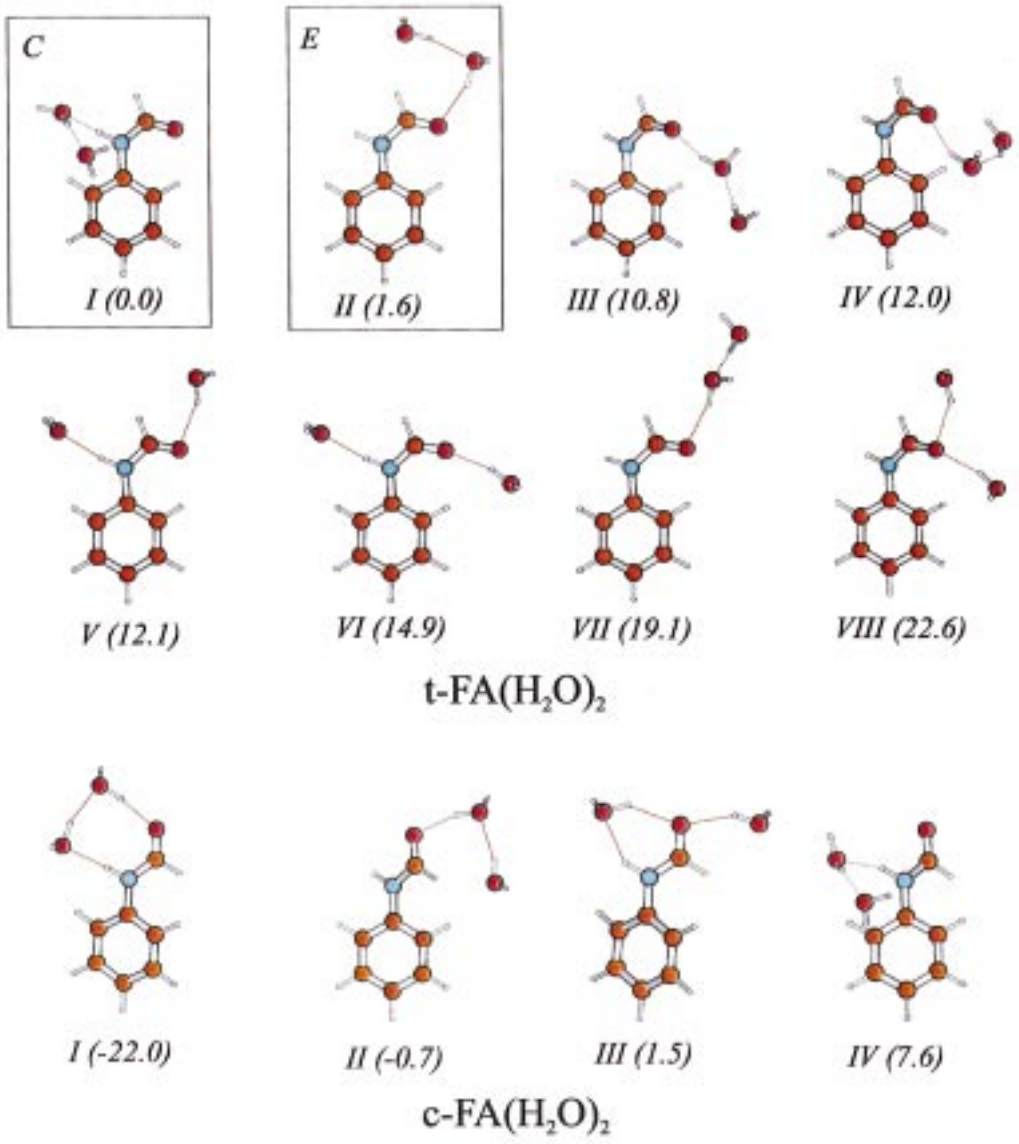

Figure 6. Stable 1:2 water clusters obtained by HF/6-31G* level geometry optimisations. The figures in parentheses are relative energies in kJ mol^{-1}, from MP2/6-31G* single-point calculations. The boxes indicate structures assigned to experimentally observed clusters C and E.

clusters. The band system labeled "C", which appears in both the $FA(H_2O)^+$ and $FA(H_2O)_2^+$ mass channels, is assigned to a 1:2 hydrated cluster. Its complex vibrational structure can be ascribed to progressions based upon three low-frequency vibrational modes (29, 38, and 51 cm^{-1}), as shown in Figure 9.

Species E shows no signal in the FA^+ or the $FA(H_2O)_2^+$ mass channels; if it were a 1:1 water cluster, then it would appear not to fragment at all, but given the fragmentation patterns of the other hydrated clusters, a more likely assignment would be to a 1:2 water cluster that loses one water molecule with 100% efficiency. The latter assignment is supported by the change in the observed relative cluster populations as the jet expansion conditions are varied. When the delay between opening the valve and arrival of the laser pulse is increased, the region of the jet expansion that is probed becomes cooler and more favorable to complex formation. In a spectrum measured using a short delay, comparatively few complexes were formed and peaks F and E appeared in the ratio 2:1. A spectrum recorded using a long delay showed evidence of extensive clustering and the peak ratio became 1:3, while the ratio of peak heights for D and F remained constant. Peak C varied in the same manner as E, supporting the assignment of both to 1:2 water clusters. The assignment is further reinforced by the rotational band contour analysis (of peak E), which will be presented in section 4.4.

Finally, the appearance of the remaining system, peak G, and its associated vibronic features in each of the $FA(H_2O)_2^+$, $FA(H_2O)_3^+$, and $FA(H_2O)_4^+$ mass channels, indicates the formation of a fifth cluster, accommodating at least four bound water molecules.

4.3. Structural Assignments of 1:1 Water Clusters. Rotational band contours of peaks D, F, and E, obtained by fluorescence excitation, are shown in Figure 10 together with optimized "best fit" contours (computed via the cross-correlation procedure described in section 2) and "ab initio" contours based on assigned structures. Extremely good agreement between the experimental contour D and the "ab initio" contour, shown in Figure 10a allows its assignment to *t*-$FA(H_2O)$ **I**, with water bound as a proton acceptor to the N−H site (see Figure 5). Likewise, band F may be assigned to the cyclic hydrate, *t*-$FA(H_2O)$ **II**, with a water proton-donating to the carbonyl oxygen.

The "ab initio" contours shown in Figure 5 are so distinctive that there is little possibility of misassigning bands D and F and a comparison of the optimized parameters with the ab initio predictions for the 1:1 clusters of formanilide bears this out (see

TABLE 5: Molecular Parameters Predicted from HF/6-31G*//MP2/6-31G*and CIS/6-31G* Calculations on Formanilide 1:2 Water Clusters

1:2 cluster	*t*-FA(H_2O)$_2$ **I**	*t*-FA(H_2O)$_2$ **II**	*t*-FA(H_2O)$_2$ **III**	*t*-FA(H_2O)$_2$ **IV**	*t*-FA(H_2O)$_2$ **V**	*t*-FA(H_2O)$_2$ **VI**	*t*-FA(H_2O)$_2$ **VII**	*t*-FA(H_2O)$_2$ **VIII**	*c*-FA(H_2O)$_2$ **I**	*c*-FA(H_2O)$_2$ **II**	*c*-FA(H_2O)$_2$ **III**	*c*-FA(H_2O)$_2$ **IV**
E_{rel}[a]/kJ mol^{-1}	0.0	1.6	10.8	12.0	12.1	14.9	19.1	22.6	−22.0	−0.7	1.5	7.6
E_{bind}[b]/kJ mol^{-1}	50.0	52.1	43.7	40.2	43.8	41.3	38.8	34.1	69.0	54.9	50.9	43.2
E_{bind}[c]/kJ mol^{-1}	37.4	39.2	30.7	22.5	32.4	29.6	28.9	20.1	54.0	40.9	36.3	30.7
E_{bind}[d]/kJ mol^{-1}	59.8	58.0	48.6	42.7	48.9	45.8	43.4	35.7	81.6	61.3	58.4	54.5
$\tau_5(C_2C_1NC_\pi)$[e]/deg	5.5	2.6	35.0	45.9	0.0	5.1	2.6	21.3	39.9	31.5	40.7	37.6
$\tau_6(C_2C_1NC_\pi)$[f]/deg	6.9	1.2	16.0	16.5	0.4	2.7	1.0	6.0	5.9	3.0	4.0	10.9
A″/MHz	990.3	2613.7	1047.5	1295.9	1295.2	896.9	2890.4	1569.1	1993.3	1922.8	1320.2	1074.0
B″/MHz	818.5	379.3	758.3	674.9	523.0	753.2	286.7	506.7	485.0	464.3	514.5	739.3
C″/MHz	520.5	332.1	471.2	528.5	373.6	411.2	271.6	386.0	400.9	376.9	384.9	519.2
A′/MHz	1003.8	2561.7	1069.8	1329.3	1295.7	886.3	2912.6	1529.9	1966.9	1943.5	1333.5	1042.2
B′/MHz	802.9	378.5	715.0	636.0	523.0	748.7	283.3	499.6	495.2	453.2	528.9	768.6
C′/MHz	492.4	330.5	442.4	502.9	373.6	407.3	268.9	378.3	399.4	368.4	380.0	500.9
$\lvert R_e\rvert \times 10^{30}$/Cm[g]	3.78	2.23	1.66	1.82	2.37	2.22	2.00	1.97	2.76	2.39	2.17	3.36
$\mu_a^2/\mu_b^2/\mu_c^2$[g]	1:85:14	5:94:1	86:10:4	82:17:1	2:98:0	97:3:0	15:82:3	53:44:3	48:41:11	10:86:4	2:75:23	17:36:47
θ_{elec}/deg[g]	+21.6	−5.3	+36.3	+61.5	−24.8	−15.8	−6.5	+19.6	−33.5	−12.4	−18.7	−18.3
r(N−H···OH_2)/pm	202.9				204.2	205.1			197.4		209.9	202.8
r(C═O···H−OH)/pm		194.9	198.4	207.1, 244.9	201.3	203.8	195.9	206.0, 211.8	192.6	194.8	206.9, 203.8	
r(H_2O−H···$C_{C=O}$)/pm		236.4			279.5		298.9	260.3		241.8	271.9	
r(H_2O···H−C_{ortho})/pm			289.9	257.7		270.2		262.4		282.0		
r(H_2O···H−C_{meta})/pm			260.9									
r(HO-H···πC_{ortho})/pm	267.5											283.4
r(H_2O···H_2O)/pm	195.6	194.1	197.2	209.7			199.7		189.0	194.2		198.5

[a] MP2/6-31G*//HF/6-31G* + 0.9(zero-point correction). Corrections taken from HF/6-31G* calculation. [b] HF/6-31G* + 0.9(zero-point correction). [c] HF/6-31G* + 0.9(zero-point correction) + BSSE correction. [d] MP2/6-31G*//HF/6-31G* + 0.9(zero-point correction + BSSE correction. Corrections taken from HF/6-31G* calculation. [e] S_0 interplane torsional angle. [f] S_1 inter-ring torsional angle (S_1 calculations at CIS/6-31G* level). [g] Transition parameters calculated at S_0 HF/6-31G* optimized geometry. θ_{elec} is defined as the TM rotation angle in the plane of the benzene ring, away from the short axis.

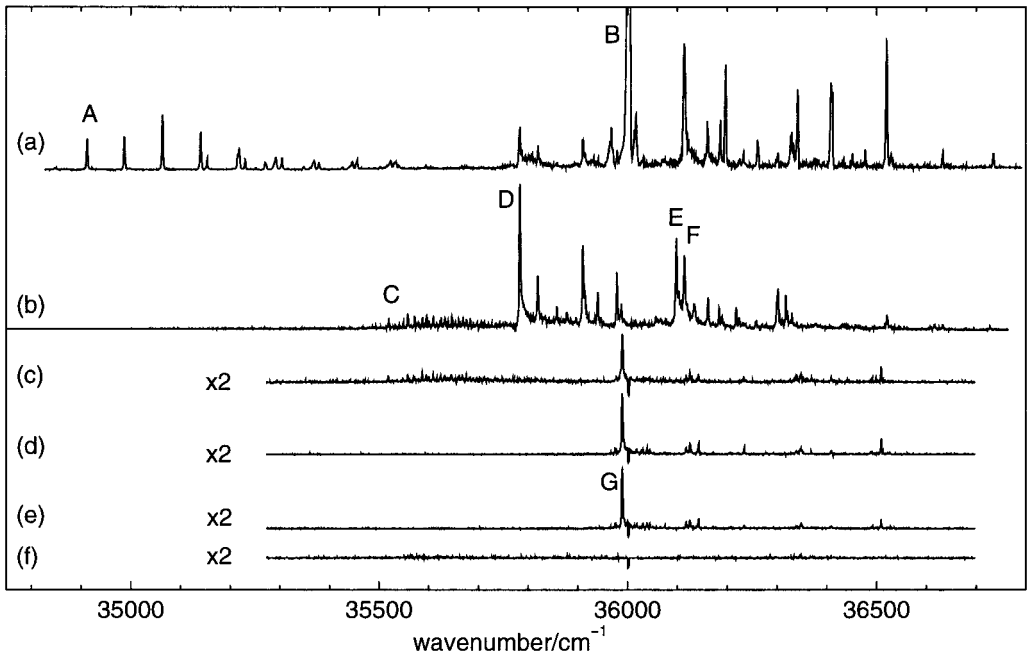

Figure 7. One-color R2PI spectra under clustering jet conditions, probing mass channels FA(H_2O)$_n^+$: (a) $n = 0$; (b) $n = 1$; (c) $n = 2$; (d) $n = 3$; (e) $n = 4$; (f) $n = 5$.

Table 6). The subband structure in band F allows a good determination of $(A-\bar{B})''$,[30] and the value obtained (0.1227 cm^{-1}) is within 1% of the value predicted for the structure, *t*-FA(H_2O) **II**. The estimated values of $\bar{B}''$ and $(B-C)''$ are also within 5% of those predicted. The a:b:c-type hybrid character determined from the optimized fit (28:65:7) is in less good agreement with the ab initio ratio (12:88:0), but both are predominantly b-type and the optimized fit is very similar to the "ab initio" contour. The lack of observed subband structure in "D" makes accurate determination of rotational constants difficult. Nevertheless, the broad shape of the band contour establishes its assignment to the structure, *t*-FA(H_2O) **I**; the optimized rotational parameters are within 7% of those predicted by ab initio methods.

The assignments of bands D and F are also consistent with the observed spectral shifts and differing extents of parent ion fragmentation. The red shift of peak "D" by 218 cm^{-1} relative to the band origin of *trans*-formanilide implies an increase in the acidity of the NH hydrogen in the electronically excited S_1 state. Hydration of the acidic hydrogen in phenol and indole results in red shifts of 353[16] and 132 cm^{-1}.[12] On the other hand, the 113 cm^{-1} blue shift of peak "F", associated with the hydrate in which a water molecule is bound at the HCO group, indicates that the carbonyl oxygen is a *weaker* proton acceptor in the S_1 state; the amide group shows a *lesser* tendency toward charge polarization in S_1 than in S_0. The increased acidity of the N−H hydrogen on electronic excitation is attributed, therefore, to an inductive effect, transferring electronic charge to the ring rather

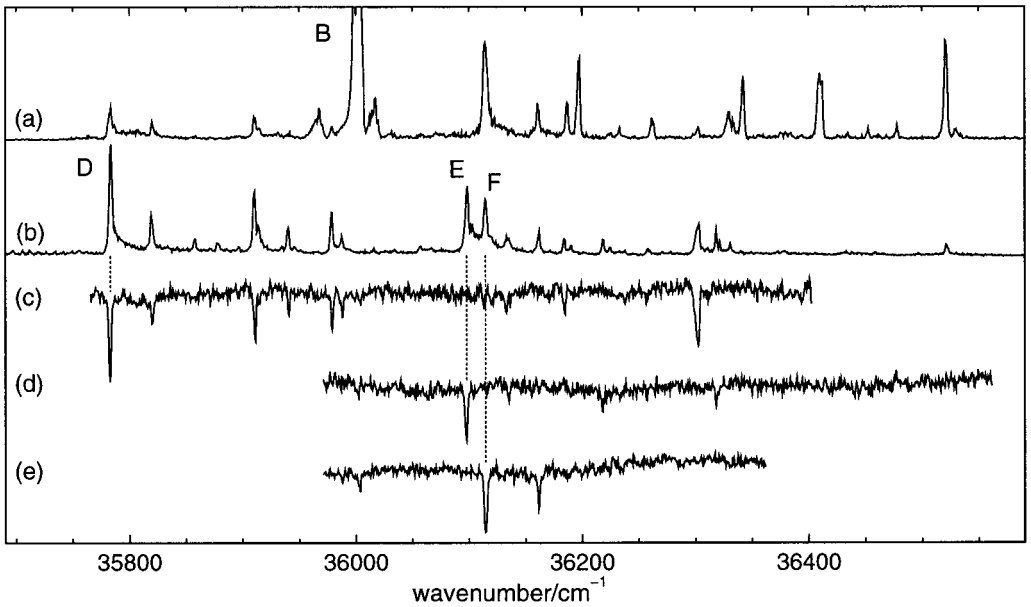

Figure 8. One-color R2PI spectra in the region of isomer "B" under clustering jet conditions: (a) mass channel FA^+; (b) mass channel $FA(H_2O)^+$. Below are R2PI hole-burning spectra probing depletion of (c) peak "D", (d) "E", and (e) peak "F".

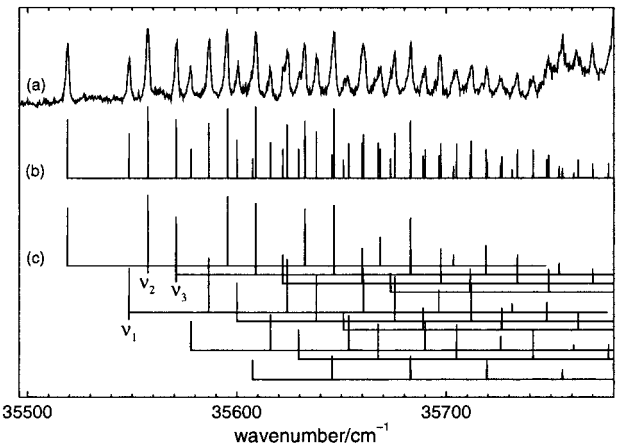

Figure 9. (a) One-color R2PI spectra in the region of peak "C" in mass channel $FA(H_2O)^+$. (b), (c) Simulated stick spectra of the progressions based on combinations of the vibrations ν_1 (29.3 cm^{-1}), ν_2 (37.7 cm^{-1}), and ν_3 (51.2 cm^{-1}).

than the carbonyl group. In the formanilide *ion*, the positive charge is distributed to some extent across the entire molecule. As a result, water molecules (as proton acceptors) at the N−H site are more strongly bound in the ion, while interactions between water hydrogens and the carbonyl oxygen are weakened. It is no surprise. therefore, to find that, following one-color ionization, cluster "D" undergoes only 25% fragmentation through dissociative loss of water, while in cluster "F" the figure is 60%.

4.4. Structural Assignments of 1:2 Water Clusters. The appearance of partially resolved subband structure in the fluorescence excitation contour of band "E", shown in the upper trace of Figure 10c, rules out all but two of the 12 possible doubly hydrated cluster structures shown in Figure 6. Only the structures, *t*-$FA(H_2O)_2$ **II** and **VII**, have $(A-\bar{B})''$ parameters large enough to show subband structure at an experimental resolution ca. 0.10 cm^{-1}. The experimental band contour of peak E is in very good agreement with the "ab initio" contour associated with the structure, *t*-$FA(H_2O)_2$ **II** (shown in the lowermost trace) and the optimized value of $(A-\bar{B})''$, 0.0737 cm^{-1}, rules out *t*-$FA(H_2O)_2$ **VII** (0.0871 cm^{-1}) in favor of *t*-$FA(H_2O)_2$ **II** (0.0753 cm^{-1}); see Table 7. The *t*-$FA(H_2O)_2$ **II** cluster, with cyclic hydrogen bonding around the HCO group, is also ca. 17 kJ mol^{-1} more stable than *t*-$FA(H_2O)_2$ **VII**, with a linear hydrogen-bonded structure. The observed position of the origin band E, blue-shifted by 97 cm^{-1} from the *trans*-formanilide origin, is consistent with its assignment to a structure in which the carbonyl oxygen acts as proton acceptor. The absence of parent ions in its R2PI spectrum, which indicates the loss of one water molecule with 100% efficiency, is also explicable given the tendency toward fragmentation in the carbonyl-bonded 1:1 cluster, "F".

Assignment of the other 1:2 cluster, system C, through rotational band contour analysis, is limited by the difficulty in obtaining a good quality contour. Its fluorescence signal was too weak to be observed, and the laser power required for R2PI detection at an adequate signal/noise level was too high to avoid some degree of saturation. The jet inlet system used to record the R2PI contour of the origin band of system C, shown in Figure 11a, also resulted in warmer rotational temperatures than in the fluorescence excitation measurements. Nonetheless, comparison of the broad shape of the experimental and ab initio band contours shown in Figure 11 does favor the assignment of system C to the structure, *t*-$FA(H_2O)_2$ **I**, shown in Figure 6 (see also the further discussion below). Fortunately, there is a great deal of additional spectral data that can also be used to greatly narrow the range of possible structural assignments. These include the position of the origin, the appearance of extended Franck−Condon progressions involving three low-frequency modes, the known frequencies of those modes, and the cluster ion fragmentation pattern.

The origin band of system C is shifted by +607 cm^{-1} from the *cis*-formanilide origin or by −482 cm^{-1} from the *trans*-formanilide origin, which represents a large spectral shift for either configuration of the formanilide host. It would be very difficult to account for a blue shift of 607 cm^{-1} in a 1:2 cluster of *cis*-formanilide. In three of the four predicted *c*-$FA(H_2O)_2$ structures, a water molecule is bound at the N-H site, and therefore red-shifted origin bands might be expected. The remaining structure, *c*-$FA(H_2O)_2$ **II**, has two water molecules bound to HCO in a fashion very similar to cluster "F", which is blue-shifted (from the *trans*-formanilide origin) by only 97

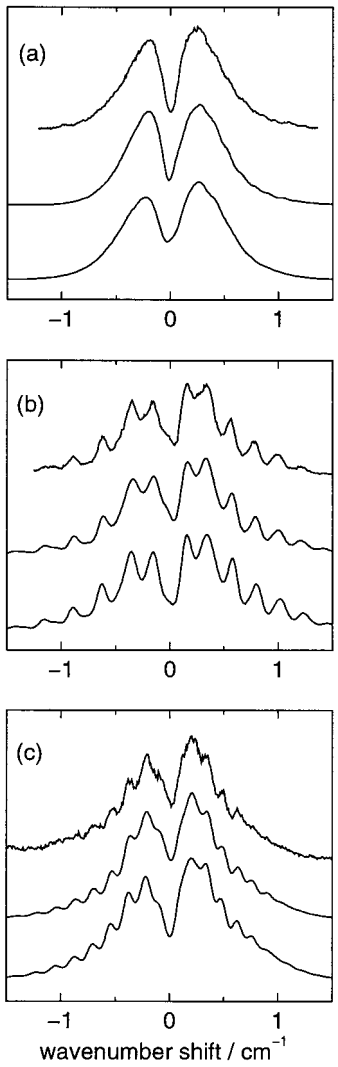

Figure 10. Upper traces: Fluorescence excitation contours of (a) band D, (b) band F, and (c) band E. Middle traces: Simulated contours obtained from correlation fits (rotational constants and hybrid band characters are given in Tables 6 and 7). Lower traces: Simulated contours based on ab initio data for (a) *t*-FA(H_2O) **I**, (b) *t*-FA(H_2O) **II**, and (c) *t*-FA(H_2O)$_2$ **II** from Tables 4 and 5.

TABLE 6: Observed and Predicted Parameters Relating to the $S_1 \leftarrow S_0$ Band Contour Fits of Formanilide 1:1 Water Clusters

	(A−$\bar{B}$)″ cm^{-1}	$\bar{B}$″ cm^{-1}	(B−C)″ cm^{-1}	$\mu_a^2/\mu_b^2/\mu_c^2$	E_{rel} kJ mol^{-1}[a]
D (35783 cm^{-1})	0.0301	0.0230	0.0114	(15:85:0)	
F (36114 cm^{-1})	0.1227	0.0163	0.0019	28:65:7	
t-FA(H_2O) **I**	0.0297	0.0247	0.0106	15:85:0	12.7
t-FA(H_2O) **II**	0.1234	0.0168	0.0020	12:88:0	16.0
t-FA(H_2O) **III**	0.0386	0.0238	0.0086	72:28:0	18.2
c-FA(H_2O) **I**	0.0729	0.0202	0.0035	13:77:10	0.0
c-FA(H_2O) **II**	0.0808	0.0174	0.0023	13:74:13	17.4

[a] MP2/6-31G*//HF/6-31G* + 0.9(zero-point correction).

cm^{-1}. On the other hand, a red-shift of 482 cm^{-1} for a *trans*-formanilide cluster would allow more possibilities. There are three *trans*-formanilide structures with at least one water molecule bound to the N−H site, *t*-FA(H_2O)$_2$ **I**, **V**, and **VI**. The clusters, *t*-FA(H_2O)$_2$ **V** and **VI**, with one water at the N−H site and the other water attached to the carbonyl oxygen, might be expected to have origins red-shifted from *t*-FA, but by no more than the 1:1 cluster, "D", *if* the effects of adding the water molecules to different sites are approximately additive. Cooperative effects in *t*-FA(H_2O)$_2$ **I** should result in strengthening of the NH···OH_2 bond and therefore enhancement of the red shift which results from the increased acidity of N−H in the S_1 state. The shortened NH···OH_2 distance in the S_1 state could also contribute to a red-shifted origin by allowing the second water molecule a slightly more favorable position over the aromatic ring. Finally, the transfer of electronic charge to the aromatic ring in the electronically excited state would strengthen the H-bonding of the second water molecule to the ring. Two of the remaining structures, *t*-FA(H_2O)$_2$ **III** and **IV**, might also conceivably produce red-shifted origins. Water molecules bridging between the carbonyl group and the ring distort the ground-state geometry of the *trans*-formanilide host considerably, resulting in dihedral angles τ_{CNCC} of 35° and 46° (see Table 5). If the energy associated with strain in the host molecule is greater in the ground state than in S_1, it would tend to shift the origin to lower wavenumber values.

The nature of the vibronic spectrum of C, with extended progressions in three low-frequency modes, suggests movement of at least one water molecule upon excitation. This discourages consideration of *t*-FA(H_2O)$_2$ **V** and **VI** but is not conclusive. Comparison of the observed vibrational frequencies (29, 38, and 51 cm^{-1}) and those predicted for the S_1 state of each of the clusters is more informative. If the criteria that predicted frequencies must be within 30% of observed values is applied, then *c*-FA(H_2O)$_2$ **I** and **II** and *t*-FA(H_2O)$_2$ **IV** may be eliminated (see Table 7).

On the basis of the reasoning above, the four remaining candidates are *t*-FA(H_2O)$_2$ **I**, **III**, **V**, and **VI**, with **I** preferred. Their relative energies at the MP2/6-31G*//HF-6-31G* level are 0.0, 10.8, 12.1, and 14.9 kJ mol^{-1}. Simulations based on each of these four structures are shown in Figure 11, along with the partially saturated contour of the origin band of C. The "ab initio" contours were calculated at 8 K because the R2PI contour of band D recorded under the same conditions was best simulated at this temperature. The appearance of band C and the ab initio relative energies both reinforce the assignment of system C to *t*-FA(H_2O)$_2$ **I**, with one water at the N−H site and the second water bound to both the first as a proton acceptor and to the π-system of the aromatic ring as a proton donor. The agreement between observed vibrational frequencies (29, 38, and 51 cm^{-1}) and those predicted ab initio (30, 43, and 50 cm^{-1}) for *t*-FA(H2O)$_2$ **I** is good (see Table 7). The reduced fragmentation efficiency of C compared with E is also consistent with the fragmentation patterns observed in the corresponding 1:1 clusters, D and F.

Finally, we note the striking similarity between the spectrum of cluster C and the indole(H_2O)$_2$ complex assigned by Zwier and co-workers.[19] Although formanilide does not consist of two adjoining rings such as indole, both systems incorporate a planar structure about the nitrogen atom: C_6H_5−NH−CH═X. The *singly* hydrated clusters of formanilide and indole, with water bound at the NH site, have spectra with strong origin bands which are red-shifted from the monomer origin by 218 and 132 cm^{-1}, respectively. The 1:2 hydrate of indole has a band origin red-shifted much further (452 cm^{-1} compared with 482 cm^{-1} for cluster C) and is associated with long intermingled progressions with vibrational frequencies of ca. 35 and 49 cm^{-1}.[12] On the basis of its resonance ion-dip infrared (RIDIR) spectrum, the 1:2 water cluster of indole was assigned to a structure almost identical to *t*-FA(H_2O)$_2$ **I** in the placement of both water molecules. The low-frequency progressions were attributed to reorientation of the water dimer following changes in the π··· HOH interaction induced by the $\pi-\pi^*$ excitation.

TABLE 7: Observed and Predicted Parameters Relating to the $S_1 \leftarrow S_0$ Band Origins of Formanilide 1:2 Water Clusters

	low-frequency vibrations/cm^{-1}[a]	(A−$\bar{B}$)″/cm^{-1}	$\bar{B}$″/cm^{-1}	(B−C)″/cm^{-1}	$\mu_a^2/\mu_b^2/\mu_c^2$	E_{rel}/kJ mol^{-1}[b]
C (35519 cm^{-1})	29.3, 37.7, 51.2					
E (36098 cm^{-1})		0.0737	0.0105	0.0012	16:77:7	
t-FA$(H_2O)_2$ **I**	29.9, 42.8, 50.4, 64.1, 98.6	0.0107	0.0223	0.0099	1:85:14	0.0
t-FA$(H_2O)_2$ **II**	23.6, 27.5, 37.7, 62.7, 86.1	0.0753	0.0119	0.0016	5:94:1	1.6
t-FA$(H_2O)_2$ **III**	10.2, 28.6, 37.8, 54.6, 75.2	0.0144	0.0205	0.0096	86:10:4	10.8
t-FA$(H_2O)_2$ **IV**	15.5, 28.1, 49.0, 70.4, 74.6	0.0232	0.0201	0.0049	82:17:1	12.0
t-FA$(H_2O)_2$ **V**	24.6, 26.4, 31.1, 49.5, 57.1	0.0283	0.0150	0.0050	2:98:0	12.1
t-FA$(H_2O)_2$ **VI**	19.1, 32.6, 35.7, 46.2, 59.5	0.0105	0.0194	0.0114	97:3:0	14.9
t-FA$(H_2O)_2$ **VII**	9.5, 13.5, 26.5, 36.5, 54.2	0.0871	0.0093	0.0005	15:82:3	19.1
t-FA$(H_2O)_2$ **VIII**	17.0, 23.0, 38.0, 46.3, 57.7	0.0374	0.0149	0.0040	53:44:3	22.6
c-FA$(H_2O)_2$ **I**	23.3, 52.1, 58.2, 70.4, 118.2	0.0517	0.0148	0.0028	48:41:11	−22.0
c-FA$(H_2O)_2$ **II**	28.1, 32.3, 36.6, 68.6, 93.5	0.0501	0.0140	0.0029	10:86:4	−0.7
c-FA$(H_2O)_2$ **III**	29.3, 39.6, 41.1, 63.1, 85.4	0.0290	0.0150	0.0043	2:75:23	1.5
c-FA$(H_2O)_2$ **IV**	22.9, 35.4, 62.7, 69.8, 91.7	0.0148	0.0210	0.0073	17:36:47	7.6

[a] Ab initio values from CIS/6-31G* calculations, scaled by 0.9. [b] MP2/6-31G*//HF/6-31G* + 0.9(zero-point correction).

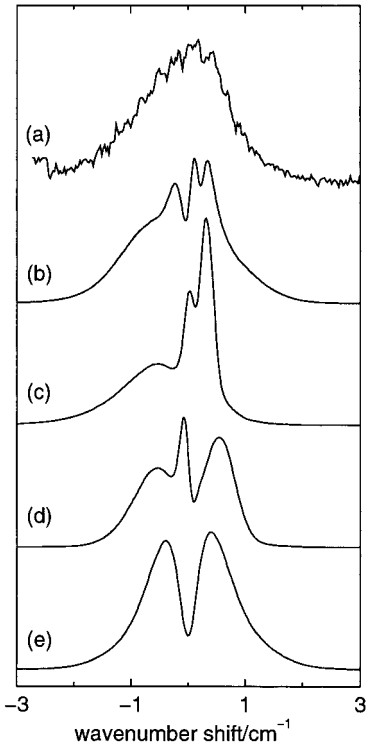

Figure 11. (a) One-color R2PI contour of band C in mass channel FA$(H_2O)^+$. Below are simulations based on ab initio data for (b) *t*-FA$(H_2O)_2$ **I**, (c) *t*-FA$(H_2O)_2$ **III**, (d) *t*-FA$(H_2O)_2$ **V**, and (e) *t*-FA$(H_2O)_2$ **VI** from Table 5 (T_{rot} = 8 K, fwhh = 0.15 cm^{-1}).

4.5. Other Water Clusters. The appearance of the remaining unassigned water cluster, band G, in the FA$(H_2O)_2^+$, FA$(H_2O)_3^+$, and FA$(H_2O)_4^+$ mass channels indicates a cluster with four (or possibly five) bound water molecules. Its vibronic spectrum is very similar to that of *trans*-formanilide, and its origin is red-shifted by only 12 cm^{-1}, strongly suggesting a trans conformation of the formanilide host. It is not possible to deduce more on the basis of the limited data, but we note that four water molecules are sufficient to form a bridge between the carbonyl and N−H sites of *trans*-formanilide, allowing formation of an extremely stable complex.

5. Discussion

All of the water features C−G have been assigned to clusters of the *trans*-formanilide, leaving the question of why clusters of the cis isomer have not been observed in R2PI scans down to 34 480 cm^{-1}. A cis conformation of the amide group allows cyclic hydrogen-bonded structures with one or two water molecules bridging between the NH and CO sites. The structures, *c*-FA(H_2O) **I** and *c*-FA$(H_2O)_2$ **I**, are the most stable 1:1 and 1:2 clusters by 12 and 22 kJ mol^{-1}, respectively, at the MP2/6-31G*//HF/6-31G* level. There is no reason they should not be *formed* in the jet expansion, and so the question becomes why are they not *detected*? One possibility is that intermolecular vibrations of the water molecule(s) couple to the torsional mode in formanilide, resulting in a broad Franck−Condon envelope of weakly allowed transitions, similar to that observed for cluster C. A further consideration is the ionization potential of the complexes. A vertical value for the ionization potential of formanilide has been reported at 8.6 eV, based on a broad feature in a low-resolution photoelectron spectrum[31] which must incorporate the overlapped contributions from both isomers. HF/6-31G* calculations of neutral formanilide indicate a large difference in vertical ionization potentials (IP_{cis} = 8.799 eV, IP_{trans} = 8.401 eV), although calculations for the ionic species show a much smaller difference in adiabatic ionization potentials ($IP_{cis} - IP_{trans}$ = 0.056 eV). If water bound at the NH site red-shifts the $S_1 \leftarrow S_0$ origin transition by a few hundred wavenumbers from the *cis*-formanilide origin at 34 912 cm^{-1}, then resonant one-color two-photon excitation will provide ca. 8.60 eV, which may barely be sufficient to ionize the complexes. More accurate data on the ionization potential of the cis isomer in particular is necessary to resolve the question.

It is noteworthy that two distinct 1:1 hydrates of *trans*-formanilide are observed, with water bound alternatively to the N−H site (cluster D) and the HCO site (cluster F). The calculated relative energies of these clusters are similar, with *t*-FA(H_2O) **I** (NH site) preferred over *t*-FA(H_2O) **II** (HCO site) by only 2 kJ mol^{-1} at the MP2/6-31G*//HF/6-31G* level (the difference increases to 6 kJ mol^{-1} with the inclusion of BSSE correction at the HF level). This is in contrast to the usual preference of water molecules for the carbonyl site of *trans*-amides. A better model for the peptide link is provided by the molecule *N*-benzyl formamide (NBFA), since it has a methylene "spacer" between the ring and the amide group. Experiments on NBFA in this laboratory reveal the presence of only one singly hydrated cluster, with water bound to the carbonyl group.[32] SCF and MP2 calculations on *N*-methylacetamide[3] using an aug-cc-pVDZ basis set indicate that the carbonyl site is preferred over the NH site by 9 kJ mol^{-1}. Formanilide differs from these two amides in the proximity of the aromatic ring, which has the effect of dramatically increasing the acidity of the N-H proton.

The two assigned 1:2 hydrates of *trans*-formanilide follow the pattern observed in the 1:1 clusters, with waters bound

alternatively to the N−H site (cluster C) and the HCO site (cluster E). Both involve cyclic hydrogen-bonded structures, in which an extra "H-bond" is formed (HOH···π_{ring} in cluster C and H_2O···HCO in cluster E). Cooperative effects are maximized in these structures since each molecule acts as both proton donor and proton acceptor. At the MP2/6-31G*//HF/6-31G* level, they are ca. 10 kJ mol^{-1} more stable than the nearest competitor, *t*-FA$(H_2O)_2$ **III** (another cyclic hydrogen-bonded structure with the water dimer bridging from the less favorable carbonyl site to the hydrogens on the ring).

In general, no evidence has been found in this study for large structural changes in amide geometry or polarization with two bound water molecules. The calculated structures of 1:2 complexes of *trans*-formanilide, which show the amide twisted relative to the aromatic ring, are far from the global potential energy minimum and are not observed experimentally. The presence of two water molecules bridging the NH site and the π-system of the ring does have a significant effect on the nature of the $S_1 \leftarrow S_0$ transition, however, resulting in a red-shifted origin with low-frequency progressions.

Further investigations of clusters C−G using the RIDIRS technique are planned to study the nature of the hydrogen-bonding interactions within them. It is also hoped that two-color REMPI measurements of ion fragmentation thresholds may provide more information about NH···OH_2 and HCO···H_2O binding energies in formanilide.

Acknowledgment. We are grateful to the Leverhulme Trust for the provision of postdoctoral support (E.G.R.) and to the EPSRC for grant support and a studentship (J.A.D.). We thank the EPSRC Laser Support Facility for the loan of the GCR200/LAS laser system critical for the two-color experiments. Finally, we are most grateful to Professor David Pratt, Dr. Romano Kroemer, and David Borst for many helpful interactions and discussions and to Peter Bellenger for his contribution.

References and Notes

(1) Guo, H.; Karplus, M. *J. Phys. Chem.* **1992**, *96*, 7273. Guo, H.; Karplus, M. *J. Phys. Chem.* **1994**, *98*, 7104.

(2) Scheiner, S. *Hydrogen Bonding—A Theoretical Perspective*; Oxford University Press: Oxford, 1997; pp 105−113.

(3) Dixon, D. A.; Dobbs, K. D.; Valenti, J. J. *J. Phys. Chem.* **1994**, *98*, 13435.

(4) Engdahl, A.; Nelander, B.; Åstrand, P.-O. *J. Chem. Phys*. **1993**, *99*, 4894.

(5) Torii, H.; Tatsumi, T.; Kanazawa, T.; Tasumi, M. *J. Phys. Chem. B* **1998**, *102*, 309.

(6) Mayne, L. C.; Hudson, B. *J. Phys. Chem.* **1991**, *95*, 2962.

(7) Larsson, K. M.; Kowalewski, J. *Spectrochim. Acta* **1987**, *43A*, 545.

(8) Chahinian, M.; Seba, H. B.; Ancian, B. *Chem. Phys. Lett*. **1998**, *285*, 337.

(9) Lovas, F. J.; Suenram, R. D.; Fraser, G. T.; Gilles, C. W.; Zozom, J. *J. Chem. Phys*. **1988**, *88*, 722.

(10) Held, A.; Pratt, D. W. *J. Am. Chem. Soc*. **1993**, *115*, 9708.

(11) Manea, V. P.; Wilson, K. J.; Cable, J. R. *J. Am. Chem. Soc*. **1997**, *119*, 2033.

(12) Tubergen, M. J.; Levy, D. H. *J. Phys. Chem.* **1991**, *95*, 2175.

(13) Connell, L. L.; Ohline, S. M.; Joireman, P. W.; Corcoran, T. C.; Felker, P. M. *J. Chem. Phys*. **1991**, *94*, 4668.

(14) Taylor, A. G.; Burgi, T.; Leutwyler, S. In *Jet Spectroscopy and Molecular Dynamics*; Hollas, J. M., Phillips, D., Eds.; Blackie Academic and Professional: London, 1995.

(15) Menapace, J. A.; Bernstein, E. R. *J. Chem. Phys*. **1987**, *87*, 6877.

(16) Abe, H.; Mikami, N.; Ito, M. *J. Chem. Phys.* **1982**, *86*, 1768.

(17) Lipert, R. J.; Colson, S. D. *Chem. Phys. Lett.* **1989**, *161*, 303.

(18) Tanabe, S.; Ebata, T.; Fujii, M.; Mikami, N. *Chem. Phys. Lett*. **1993**, *215*, 347.

(19) Carney, J. R.; Hagemeister, F. C.; Zwier, T. S. *J. Chem. Phys*. **1998**, *108*, 3379.

(20) Dickinson, J. A.; Joireman, P. W.; Randall, R. W.; Robertson, E. G.; Simons, J. P. *J. Phys. Chem. A* **1997**, *101*, 513. Joireman, P. W.; Kroemer, R. T.; Pratt, D. W.; Simons, J. P. *J. Chem. Phys.* **1996**, *105*, 6075.

(21) Dickinson, J. A.; Hockridge, M. R.; Kroemer, R. T.; Robertson, E. G.; Simons, J. P.; McCombie, J.; Walker, M. *J. Am. Chem. Soc*. **1998**, *120*, 2622.

(22) Hockridge, M. R.; Robertson, E. G. *J. Phys. Chem. A*, in press.

(23) Hockridge, M. R.; Knight, S. M.; Robertson, E. G.; Simons, J. P.; McCombie, J.; Walker, M. *Phys. Chem. Chem. Phys.* **1999**, *1*, 407.

(24) Hockridge, M. R.; Robertson, E. G.; Simons, J. P. *Chem. Phys. Lett*. **1999**, *302*, 538.

(25) Kroemer, R. T.; Liedl, K. R.; Dickinson, J. A.; Robertson, E. G.; Simons, J. P.; Borst, D. R.; Pratt, D. W. *J. Am. Chem. Soc*. **1998**, *120*, 12573.

(26) Dickinson, J. A.; Joireman, P. W.; Kroemer, R. T.; Robertson, E. G.; Simons, J. P. *J. Chem. Soc., Faraday Trans*. **1997**, *93*, 1467.

(27) Elkes, J. M. F.; Robertson, E. G.; Simons, J. P.; McCombie, J.; Walker, M. *Phys. Chem. Commun.* **1998**, *1*.

(28) Frisch, M. J.; Trucks, G. W.; Schlegel, H. B.; Gill, P. M. W.; Johnson, B. G.; Robb, M. A.; Cheeseman, J. R.; Keith, T.; Petersson, G. A.; Montgomery, J. A.; Raghavachari, K.; Al-Laham, M. A.; Zakrzewski, V. G.; Ortiz, J. V.; Foresman, B.; Cioslowski, J.; Stefanov, B. B.; Nanayakkara, A.; Challacombe, M.; Peng, C. Y.; Ayala, P. Y.; Chen, W.; Wong, M. W.; Andres, J. L.; Replogle, E. S.; Gomperts, R.; Martin, R. L.; Fox, D. J.; Binkley, J. S.; Defrees, D. J.; Baker, J.; Stewart, J. P.; Head-Gordon, M.: Gonzalez, C.; Pople, J. A. *Gaussian 94*, revision C.3; Gaussian, Inc.: Pittsburgh, PA, 1995.

(29) Hollas, J. M.; Ridley, T. *Chem. Phys. Lett*. **1980**, *75*, 94.

(30) The band contour analyses were based on a rigid rotor Hamiltonian. While hydrogen bonding between water and formanilide allows flexibility and even large amplitude motions of water in some clusters, these effects are not apparent in the rotationally cool and partially resolved contours presented here.

(31) Zverev, V. V. *Izv. Akad. Nauk SSSR, Ser. Kim.* **1992**, *3*, 602.

(32) Hockridge, M. R.; Robertson, E. G.; Simons, J. P. Rutherford Appleton Laboratory Central Laser Facility Annual Report 1997/98; p 71.